

Supplemental Information

Revvng an engine of human metabolism: Activity enhancement of Triocephosphate Isomerase via hemi-phosphorylation

Luis F. Schachner¹, Benjamin Des Soye^{1,2}, Soo Ro³, Grace E. Kenney^{3,4}, Ashley N. Ives¹, Taojunfeng Su¹, Young Ah Goo¹, Michael C. Jewett², Amy C. Rosenzweig³, and Neil L. Kelleher^{1,3*}

¹ Department of Chemistry, the Proteomics Center of Excellence, Northwestern University, Evanston, IL, 60208, USA

² Department of Chemical and Biological Engineering, Northwestern University, Evanston, IL, 60208, USA

³ Department Molecular and Biological Sciences, Northwestern University, Evanston, IL, 60208, USA

⁴ Department of Chemistry, Harvard University, Cambridge, MA, 02140, USA

Corresponding author: Neil Kelleher, n-kelleher@northwestern.edu

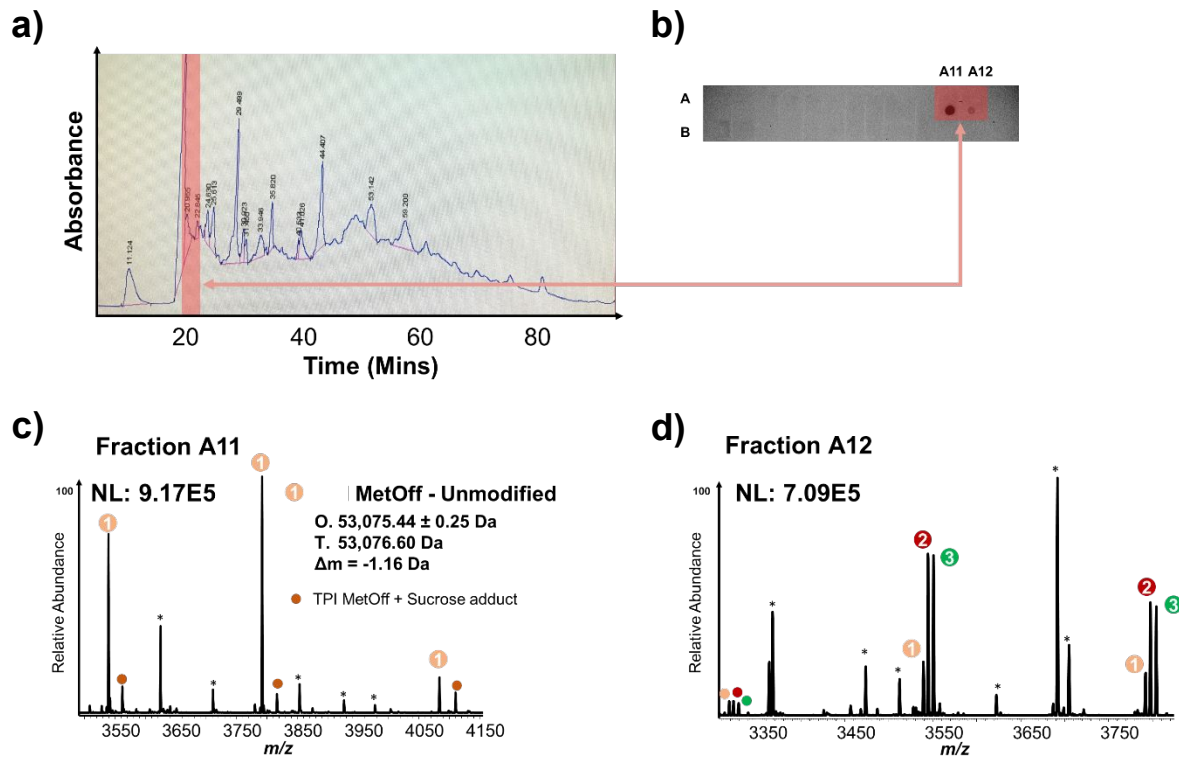
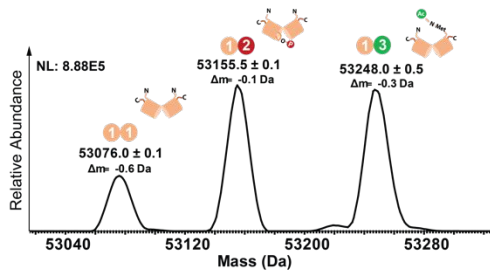
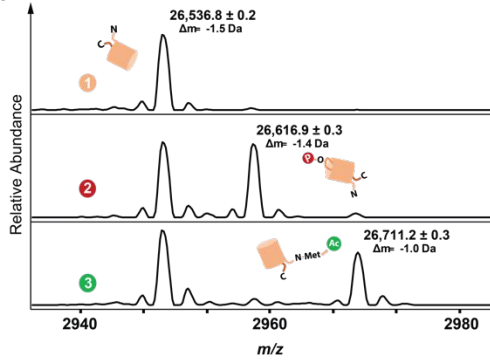


Figure S1. HEK whole cell lysates were fractionated into 96-well plates by ion exchange with an ammonium acetate gradient. Panel **(A)** contains the ion exchange chromatographic trace, where intensity reflects 280 nm absorbance. Upon fractionation into a 96-well plate, each well was dotted onto a nitrocellulose membrane and immunoblotted using anti-TPI antibody (Abcam; ab96696), as shown in panel **(B)**. The TPI-containing fractions A11 and A12 were analyzed by native MS, as shown in the MS1 spectra of panels **(C)** and **(D)**. NL values reflect the maximum signal intensity in the spectrum. In Panel (d), numbers 1 (unmodified), 2 (phosphorylation), and 3 (N-terminal acetylation) in the colored circles correspond to the complexes identified in **Fig. 1A** and **Fig. S2**. Asterisks (*) are placed above the peaks of unidentified proteins.

a) Native MS of TPI Dimers from HEK 293 Cells (MS¹)

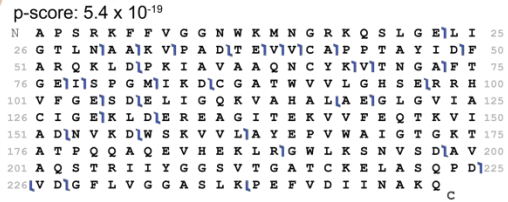


b) Monomer Ejection Experiment (MS²)

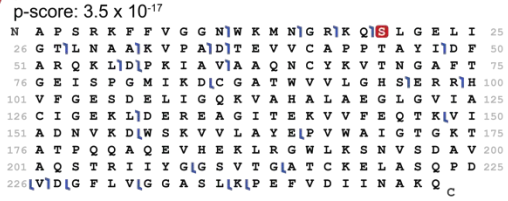


c) Fragmentation of Ejected Monomers (MS³)

1 Unmodified, Met-OFF TPI



2 pSer20 TPI



3 Nt-Acetylated, Met-ON TPI



Figure S2. Native Top-Down Mass Spectrometry (nTDMS) performed on endogenous TPI dimers from HEK293 cells identifies PTMs in a site-specific manner.

(A) The nTDMS platform first consists of the measurement of the average mass of the intact multi-proteoform complexes (MPCs) of TPI (MS¹). **(B)** In the second step, a single charge state of each complex is isolated and collisionally activated with nitrogen gas to eject monomers (MS²). In this way, the subunits that make up each intact MPC are liberated and characterized (calculated average masses are provided). Shown in the panel are single charge states of the liberated subunits for each MPC activated. When activating MPC (1-1), only one type of subunit is ejected, indicating that the intact MPC is a homodimer. Upon activation of MPC (1-2) and (1-3), two different subunits are ejected indicating that MPCs (1-2) and (1-3) are each heterodimers. **(C)** In the third step, TPI dimers are dissociated in the electrospray source, and each ejected subunit is isolated and subjected to further vibrational activation via collisions with neutral gas (HCD). This process yields backbone fragmentation products from each monomer (pseudo-MS³), which are depicted as blue flags in the three graphical fragment maps. Each flag indicates the segments of the protein sequence that are accounted for in mass by fragmentation, thereby enabling the identification of proteoforms and the

localization of their modifications (red, phosphorylation; green, acetylation). Met-Off indicates removal of initiator methionine; Met-On indicates retention of initiator methionine. The TPI proteoforms were identified with the following p-scores: (1) 5.4×10^{-19} ; (2) 3.5×10^{-17} ; (3) 3.7×10^{-9} .

A note on TPI residue numbering

All human TPI residue numbering in the manuscript is based on the TDMS-validated endogenous sequence, which differs from the canonical TPI on UniProt (P60174-1) by lacking the initiator Met. Consequently, Ser21 in the UniProt sequence for example is labeled as Ser20 in the manuscript. Other references use isoform 2 (P60174-3) as the basis for residue numbering which contains an additional 37 residues. However, this endogenous TPI proteoform was not observed in this study.

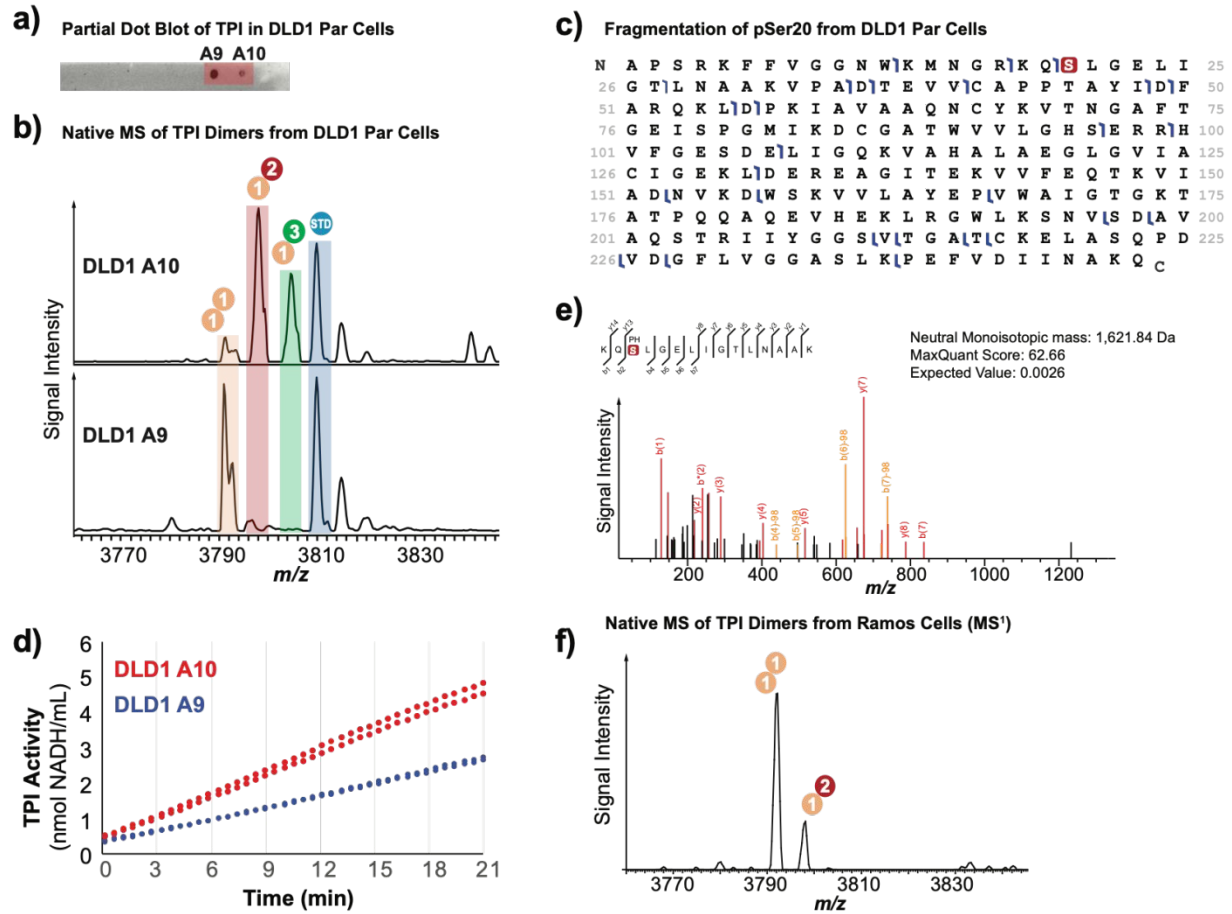


Figure S3. Proteomic data from cell lines on pSer20 TPI. **(A, B)** Dot blot showing two chromatographically separated fractions of DLD1 cell line lysate containing TPI, with their corresponding MS readout demonstrating the presence of the TPI dimer 1-2, made up of the phospho-TPI proteoform. **(C)** nTDMS fragmentation of phospho-TPI showing localization to Ser20. **(D)** TPI activity assay of the TPI-containing fractions, normalized for TPI concentration. **(E)** Digestion-based proteomics analysis showing localization of phosphorylation to Ser20. **(F)** MS readout showing phospho-TPI present in the Ramos cell line.

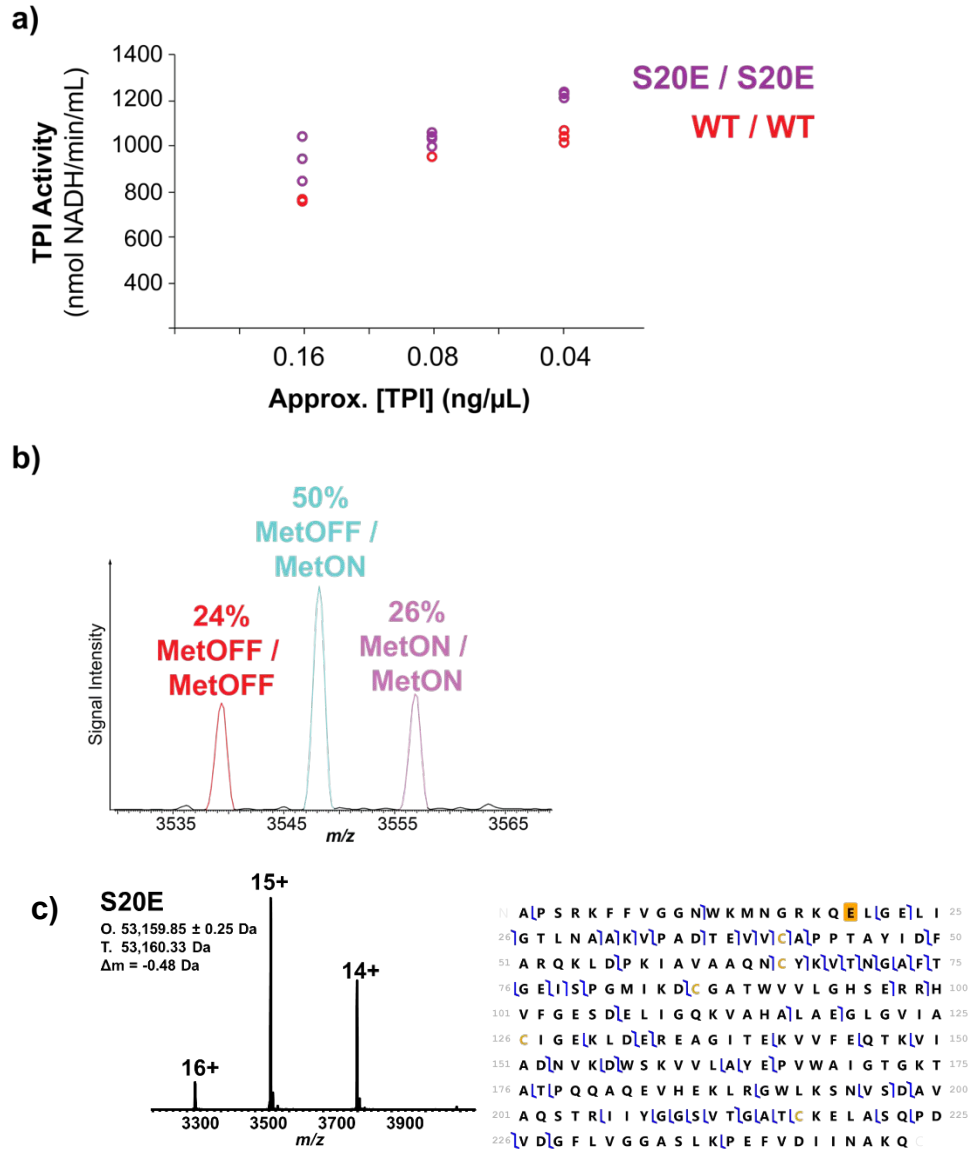


Figure S4. (A) TPI activity measurement of WT/WT and S20E/S20E homodimers reflect comparable enzymatic activities. **(B)** As a control, Methionine-tagged TPI and WT (Met-Off) TPI were mixed 1:1, denatured and refolded. The obtained 1:2:1 ratio for the three recombined dimers reflects a stochastic distribution where homo- and hetero-dimerization are equally likely. **(C)** nTDMS characterization of S20E TPI mutant generated by CFPS. Left panel contains an MS¹ of the S20E TPI dimer and on the right, the graphical fragment map of the ejected subunit with the S20E mutation highlighted in yellow.

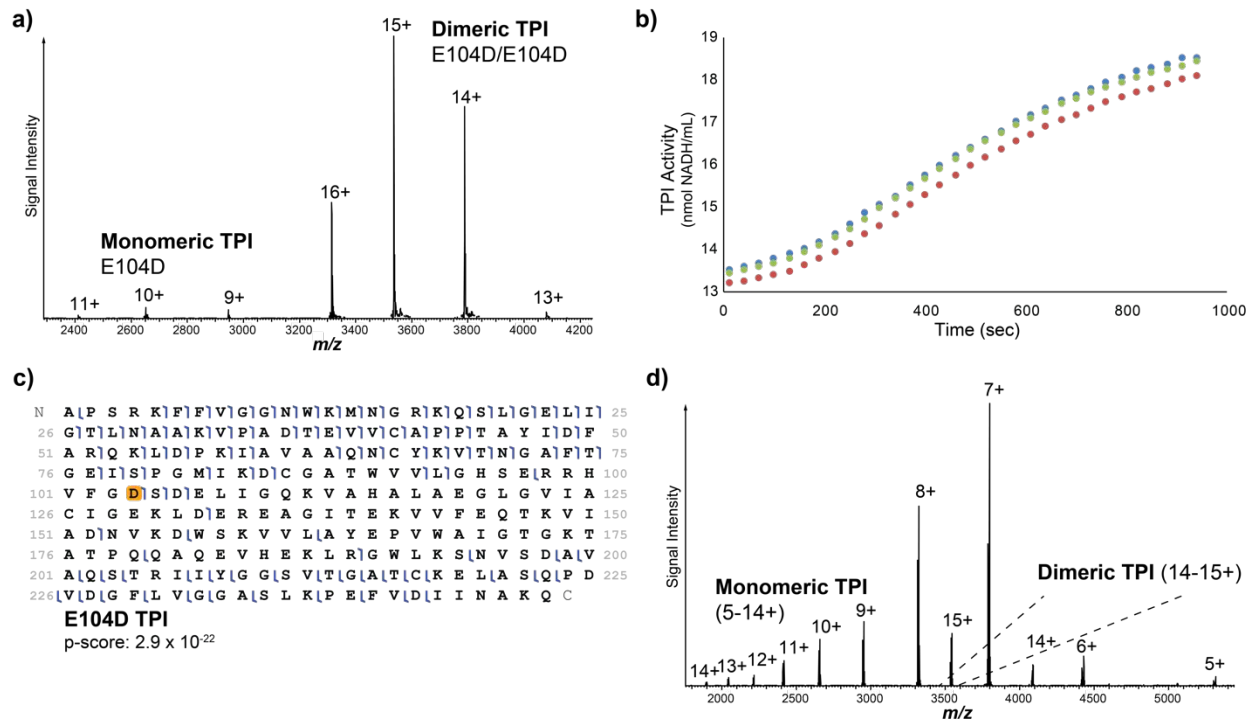


Figure S5. E104D mutant can homodimerize but does not fully re-dimerize after chemical denaturation. **(A)** Intact native mass spectrometry, **(B)** activity study and **(C)** graphical fragmentation map of the E104D TPI mutant. **(D)** After denaturation and refolding, native mass spectrometry revealed that the E104D TPI does not fully dimerize as observed for the WT counterpart of TPI.

Supplemental Discussion on E104D TPI point mutant, which can dimerize but does not fully refold after denaturation.

Interested in understanding the dimerization properties of TPI, we created the E104D mutant associated with TPI-deficiency disorder.³³ This TPI mutant has similar catalytic activity to WT but is known to contain an altered water network at the dimer interface, lower thermostability and impaired dimer formation.^{32, 34} Our MS and kinetic analyses confirmed the formation of catalytically active E104D homodimer (**Fig. S5A-C**). Intriguingly, monomeric E104D TPI was detected by native MS without any added activation energy. Moreover, the E104D monomer did not refold after denaturation and its MS charge state distribution became denatured-like, resembling that of an intrinsically disordered protein³⁵ (**Fig. S5D**).

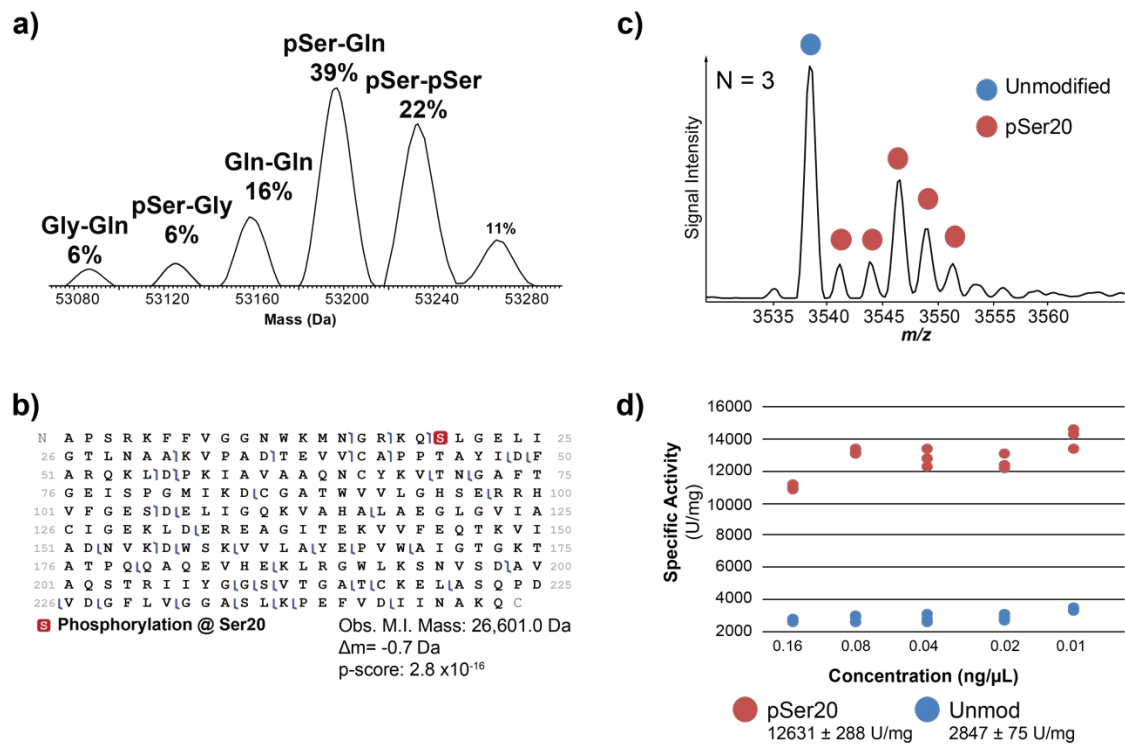


Figure S6. pSer20 containing TPI dimers are >4 fold more active. **(A)** Native MS analysis of TPI dimers containing pSer20 and mutant dimers generated by mis-incorporation of Gln and Gly during cell-free proteoform synthesis (CFPS). **(B)** Native Top-Down MS fragmentation of pSer20-TPI, confirming the presence and localization of the phospho-Serine after CFPS. **(C)** MS readout of WT-TPI (blue) spiked into the CFPS sample (red, containing pSer20) at various concentrations in order to normalize their concentration prior to concentration-sensitive kinetic analyses. **(D)** TPI activity assay of the material characterized in panel (C) comparing the specific activity (U/mg) of pSer20-containing samples relative to unmodified, WT TPI.

e) S20Q

1 A P S R K F F V G G N W K M N G R K Q **Q** L G E L I 25 O. 26,562.04
26 **G** T L N A A K V P A D T E V V C A P P T A Y I D F 50 T. 26,562.73 Da
51 A R Q K L D P K I A V A A Q N C Y K V T N G A F T 75 $\Delta m = -0.69$ Da
76 **G** E I S P G M I K D C G A T W V V L G H S E R R H 100
101 V F G E S D E L I G Q K V A H A L A E G L G V I A 125
126 C I G E K L D E R E A G I T E K V V F E Q T K V I 150
151 A D N V K D W S K V V L A Y E P V W A I G T G K T 175
176 A T P Q Q A Q E V H E K L R G W L K S N V S D A V 200
201 A Q S T R I I Y G G S V T G A T C K E L A S Q P D 225
226 V D L G F L V G G A S L K P E F V D I I N A K Q

f) S20G

1 A P S R K F F V G G N W K M N G R K Q **G** L G E L I 25 O. 26,490.96
26 **G** T L N A A K V P A D T E V V C A P P T A Y I D F 50 T. 26,491.69 Da
51 A R Q K L D P K I A V A A Q N C Y K V T N G A F T 75 $\Delta m = -0.73$ Da
76 **G** E I S P G M I K D C G A T W V V L G H S E R R H 100
101 V F G E S D E L I G Q K V A H A L A E G L G V I A 125
126 C I G E K L D E R E A G I T E K V V F E Q T K V I 150
151 A D N V K D W S K V V L A Y E P V W A I G T G K T 175
176 A T P Q Q A Q E V H E K L R G W L K S N V S D A V 200
201 A Q S T R I I Y G G S V T G A T C K E L A S Q P D 225
226 V D L G F L V G G A S L K P E F V D I I N A K Q

Figure S6 (continued). Graphical fragment maps of TPI proteoforms with mis-incorporated amino acids during generation by cell-free proteoform synthesis. Each dimer present in the mixture was isolated and activated to eject proteoforms that were then fragmented for complete molecular characterization. Panels (E) and (F) contain the graphical fragment maps that characterize the sequence and modifications of each proteoform generated by CFPS. The observed and theoretical monoisotopic masses are provided for each proteoform.

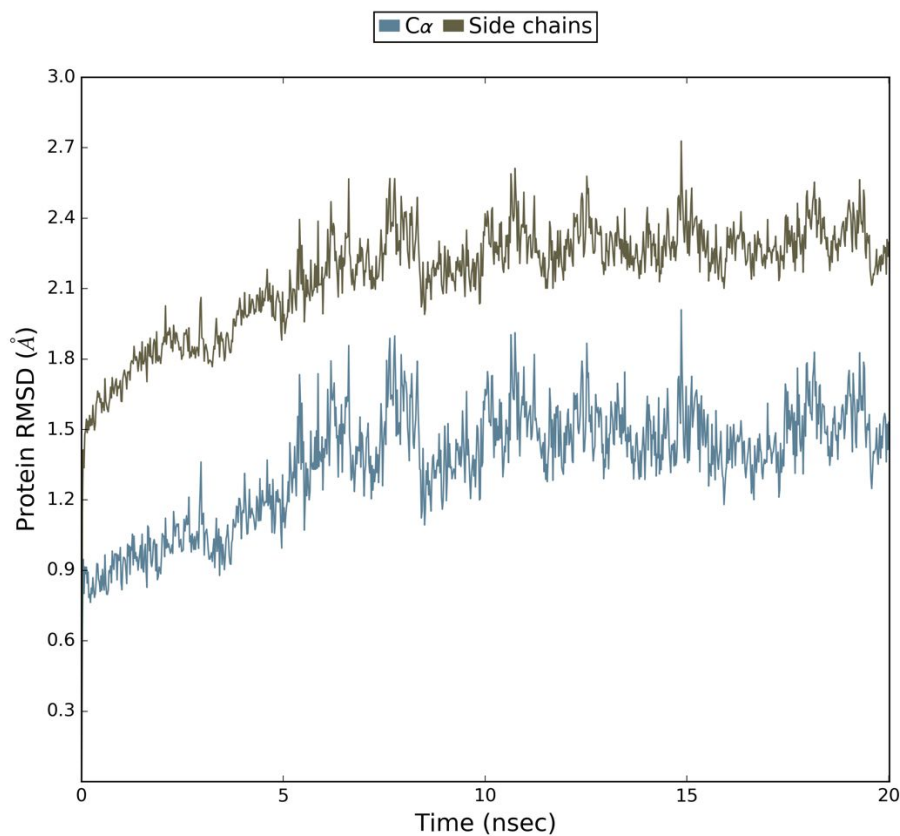


Figure S7. Root Mean Square Deviation (RMSD) evolution of pSer20-TPI (left Y-axis) during 20 ns molecular dynamics simulation at 300 K. The RMSD measurement reflects the average change in displacement of pSer20-TPI atoms with respect to the wild-type structure (PDB: 4POC).

Substrate docking energetic parameters calculated from the simulation:

	Phosphorylated	Non-Phosphorylated
ΔG	-13.52 kcal/mol	-4.28 kcal/mol
Strain Energy (Penalty)	1.56 kcal/mol	11.25 kcal/mol

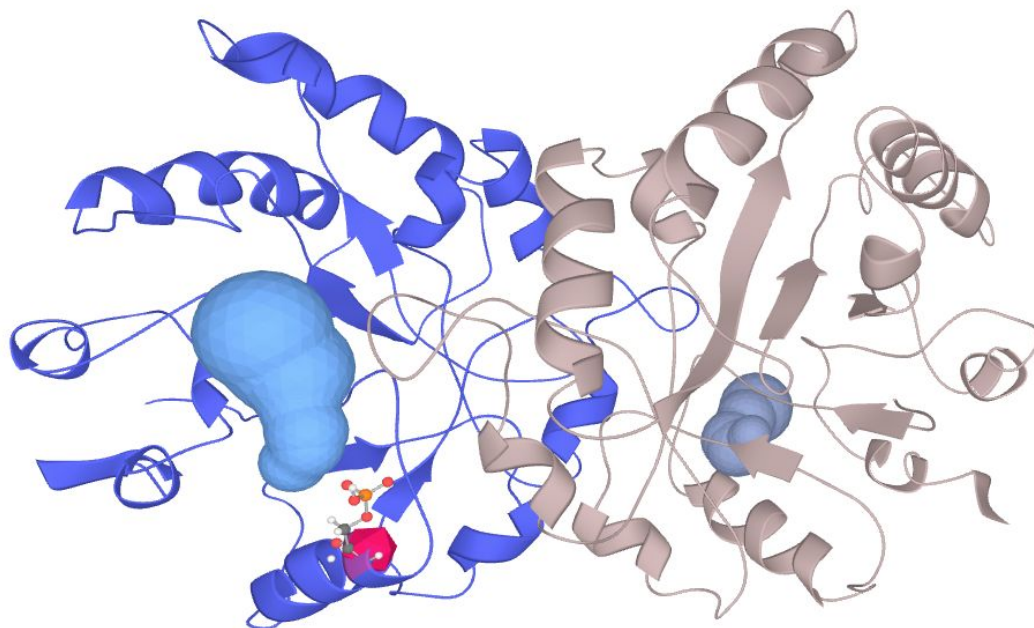


Figure S8. Prediction of tunnels in the simulated TPI-pSer20 model. The MoleOnline server (<https://mole.upol.cz/>) was used to calculate tunnels in the sTPI-pS20 model and TPI WT structure. Tunnels present in sTPI-pS20 but not found in WT are highlighted in blue and gray. The monomer housing pSer20 is colored in blue. The blue tunnel is predicted to be 10 Å long with a volume of 2548 Å³. The pSer20 residue is depicted as ball and sticks.

For an opportunity to assess the channel that forms in the simulated TPI-pSer20 model in augmented reality, scan the following QR code with a smartphone, download the Adobe Aero app, and follow the on-screen instructions.



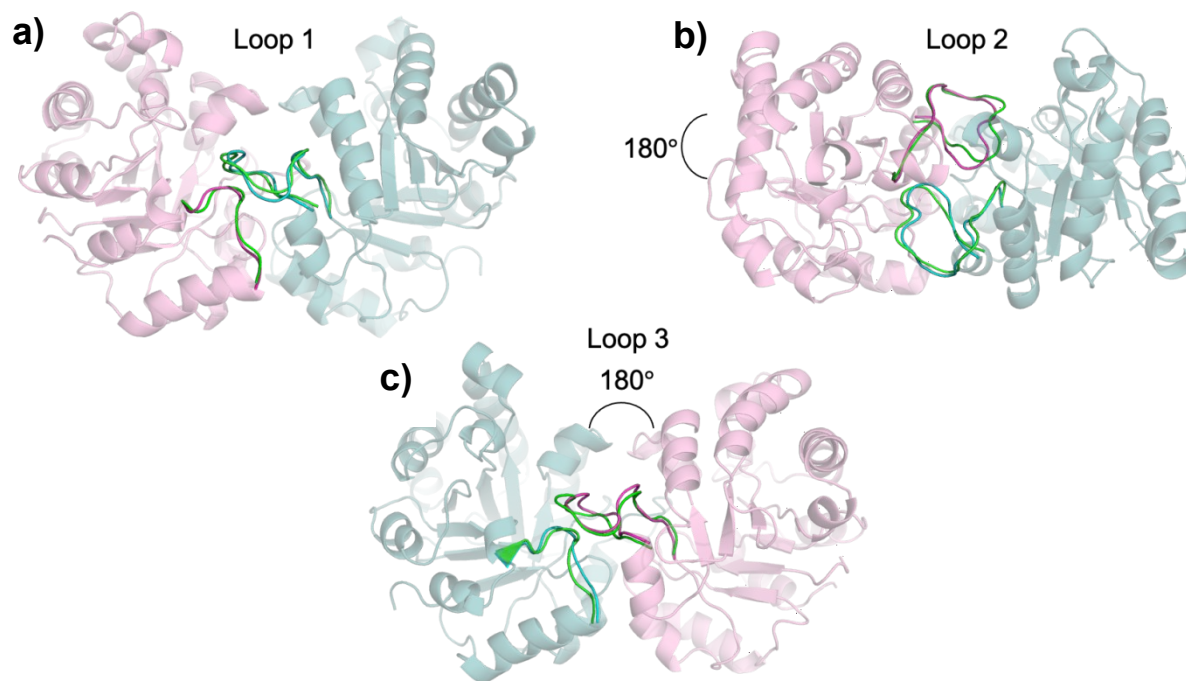


Figure S9. Loop regions at the TPI dimer interface. The phosphorylated subunit of sTPI-pSer20 is colored in pink and the unphosphorylated subunit is colored in blue. The TPI-WT loops are colored in green. The loop regions 1-3 in the dimer interface is shown in **(A)** front view, **(B)** top view, and **(C)** 180° view.

Supplemental Structural Analysis of sTPI-pSer20.

In loop 1, four hydrogen bonding interactions observed in the WT structure are absent in the pS20 model, but a new bond (Asn71/OD1 - Arg17/NH2) is observed (**Table S2, Fig. S8**). Additionally, in the WT structure, loop 3 is symmetrical to loop 1 (opposite each other at the dimer interface) and maintains the same hydrogen bonding interactions as loop 1. However, in the sTPI-pSer20 structure, the symmetry shared between loop 1 and loop 3 is not present, in which loop 1 H-bonds are different from those of loop 3. The two symmetric hydrogen bonds in TPI-WT loop 2 (Gly76/N(H) - Gln64/OE1, Gln64/OE1-Gly76/N(H)) are perturbed in the sTPI-pSer20 with the loss of the Gly76/N(H) – Gln64/OE1 interaction (**Table S2, Figure S9**). Overall, the simulated TPI-pSer20 model suggests that the structural changes near the hemi-phosphorylation site and the hydrogen

bonds at the dimer interface break the symmetrical interactions between the two monomers. The change in symmetry at the dimer interface results in further structural perturbations throughout the structure. In the loop region (Val231-Pro238) near the substrate binding site, Leu236 is shifted 100° away from the substrate pocket and toward the solvent area, opening a cavity for the substrate (**Fig. 2E**). These perturbations induced the formation of a channel that guides the substrate into the active site (**Fig 2F**, at right).

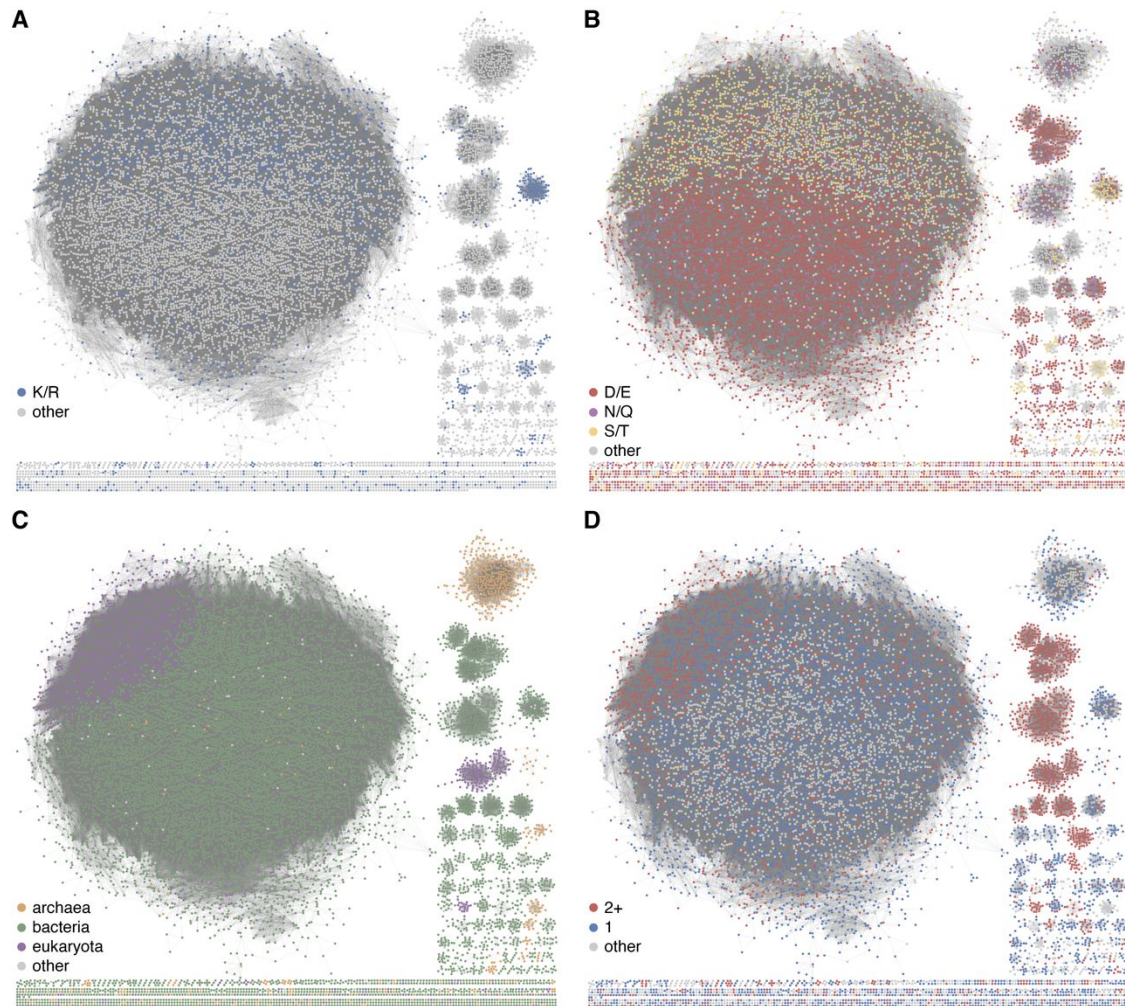


Figure S10. Sequence similarity network analysis for 56,000 TPIs. This sequence similarity network (SSN) was visualized with representative nodes chosen at 70% identity and an expectation value cutoff of $1E-70$. **(A)** SSN nodes colored by the identity of the residue at the position of pSer20. **(B)** Conservation of residues at the position of Lys18. The presence of an acidic sidechain (Lys, occasionally Arg) is highly (though not exclusively) correlated with the presence of a Ser at the position of Ser20. **(C)** SSN colored by superkingdom membership. While the distribution of serine residues is not limited to eukaryotic TPI proteins, prokaryotes predominantly have an acidic (Glu or, more rarely, Asp) sidechain at that position, and the presence of serine is seen primarily in eukaryotes and a smaller subset of prokaryotes. **(D)** Many species have more than one form of TPI, including not only alternate isoforms in eukaryotes but second homologs in prokaryotes.

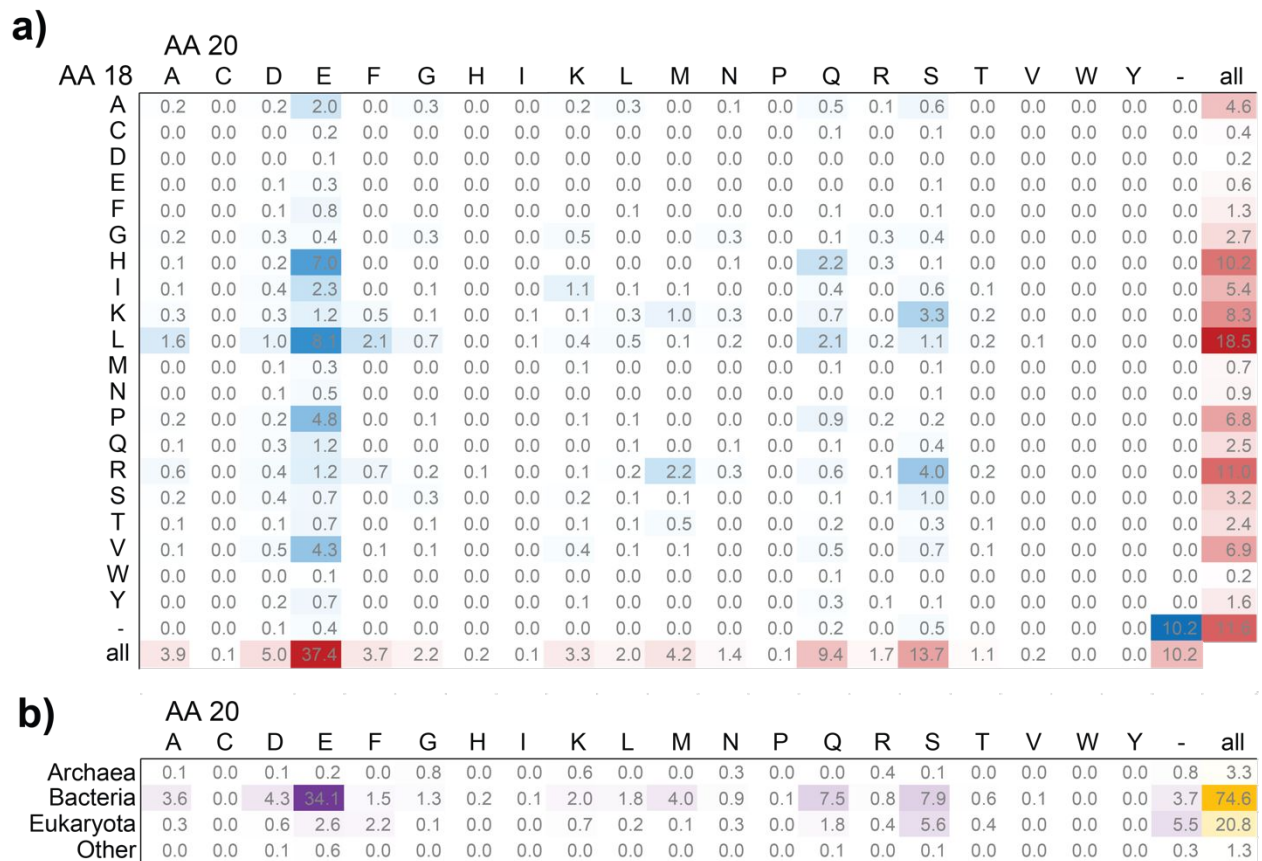


Figure S11. (A) Matrix of co-occurrence for residues at positions 18 and 20. Values represent percent of total sequences with a given residue pair. Basic residues (Arg and Lys) are strongly preferred when Ser is at position 20, but not when an acidic residue (Asp or Glu) is present. Absolute abundance of an amino acid at a given position is in red. **(B)** Occurrence of residues at position 20 by superkingdom. Serine is the preferred option at position 20 in eukaryotes but not other kingdoms of life.

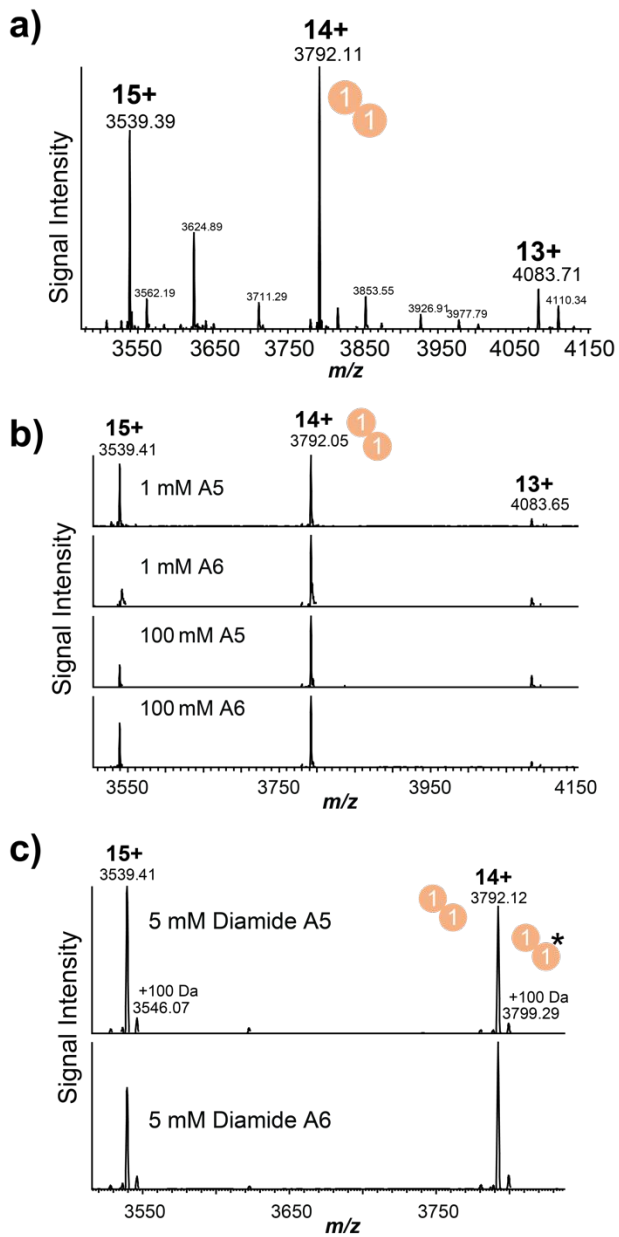


Figure S12. Control native mass spectra, showing identification of unmodified TPI in lysate fractions **(A)** from control HEK cells, **(B)** HEK cells treated with 1 and 100 mM hydrogen peroxide, and **(C)** HEK cells treated with 5 mM diamide.

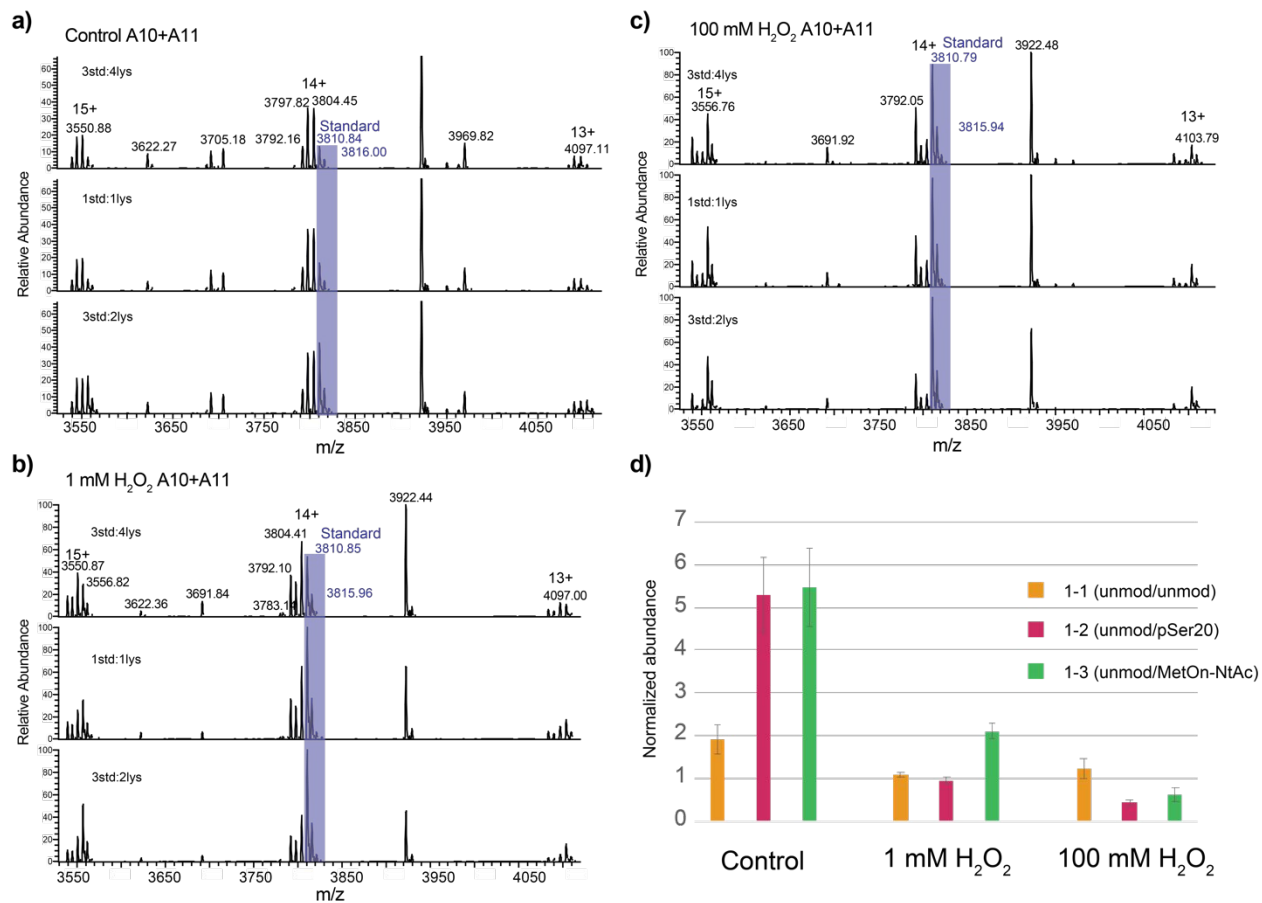
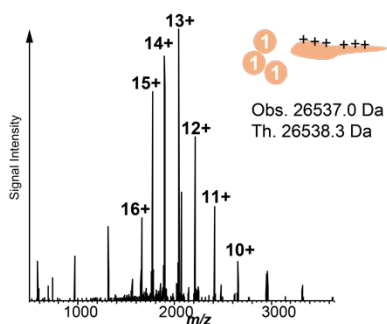


Figure S13. Native mass spectra of TPI dimers from **(A)** Control HEK cells, **(B)** HEK cells treated with 1 mM hydrogen peroxide, and **(C)** HEK cells treated with 100 mM hydrogen peroxide. Each spectrum contains the distribution of TPI dimers described in main text **Fig. 6** with a spiked-in Methionine-tagged TPI standard (Met-TPI) at three different ratios (blue stripe). **(D)** Quantitation of the relative abundance of the endogenous TPI dimers after normalizing each dimer's intensity to the intensity of Met-TPI standard spiked into the sample.

a) Ejected TPI Subunit from 16+ tetramer (MS²)



b) Fragmentation Identifies Ejected TPI Subunit (MS³)



Figure S14. (A) TPI subunit ejected from tetramer upon collisions with nitrogen gas. **(B)** Data obtained from a native top-down MS fragmentation experiment on the ejected TPI monomer, identifying it as the unmodified, Met-Off proteoform.

Table S1. Hydrogen bonding distances of S20E residue to water ions in S20E-TPI crystal structure.

	H-bonding distance (Å)
Glu20/OE1 – H2O	2.8
Glu20/OE1 – H2O	2.5
Glu20/OE1 – H2O	2.9
Glu20/OE2 – H2O	2.8
Glu20/OE2 – H2O	2.6
Glu20/OE2 – H2O	2.5
Glu20/OE2 – H2O	2.6

Table S2. Hydrogen bonding distances of residues in loops 1-3 of TPI-WT crystal structure and simulated TPI-pSer20.

TPI-WT dimer loop 1		
Chain A	Chain B	H-bonding distance (Å)
Asn71/OD1	Gly16/N(H)	2.8
Asn71/OD1	Arg17/NH1	2.2
Gly72/N(H)	Met14/O	2.1
Gly72/O	Met14/N(H)	2.4
Thr75/OG1	Asn11/NH2	2.3
Thr70/O	Arg17/NH2	2.1
Thr70/OG1	Arg17/NH2	2.6
sTPI-pS20 loop 1		
Asn71/OD1	Arg17/NH2	1.9
Asn71/OD1	Arg17/NH1	2.1
Gly72/N(H)	Met14/O	2.0
Thr70/OG1	Arg17/NH2	2.4

TPI-WT dimer loop 2		
Chain A	Chain B	H-bonding distance (Å)
Gly76/N(H)	Gln64/OE1	1.9
Gln64/OE1	Gly76/N(H)	2.0
sTPI-pS20 loop 2		
Gln64/OE1	Gly76/N(H)	2.0

TPI-WT dimer loop 3		
Chain A	Chain B	H-bonding distance (Å)
Asn11/ND2(H)	Thr75/OG1	2.2
Met14/N(H)	Gly72/O	2.4
Met14/O	Gly72/N(H)	2.0
Gly16/N(H)	Asn71/OD1	2.6
Arg17/NH1	Asn71/OD1	2.1
Arg17/NH2	Thr70/O	2.2

Arg17/NH2	Thr70/OG1	2.6
sTPI-pS20 loop 3		
Asn15/ND2(H)	Gly72/O	2.2
Met14/O	Gly72/N(H)	2.1
Gly16/N(H)	Asn71/OD1	2.6
Arg17/NH1	Asn71/OD1	2.1
Arg17/NH1	Thr70/O	2.6
Arg17/NH2	Thr70/O	1.9
Arg17/NH2	Thr70/OG1	2.2